Influence of atmospheric turbulence on imaging quality of electro-optical sensors in different climates

Karin R. Weiss-Wrana
FGAN-FOM, Gutleuthausstraße 1, D 76275 Ettlingen, Germany
Doc.:FGAN-FOM 2003/11

ABSTRACT

During long-term experiments FGAN-FOM measured C_n^2 values over land with identical scintillometers in two different climates, in moderate climate in mid-Europe and in arid climate. Since C_n^2 usually changes as a function of time-of-day and of season its influence on electro-optical systems can only be expressed in a statistical way. The cumulative frequencies of occurrence were calculated for a time period of one month for different times of the day.

The statistical analysis was applied to calculate the effects of atmospheric turbulence on sensor performance like turbulence MTF, the resolution limit due to turbulence and intensity fluctuation. The calculations were performed for a SWIR sensor (active imaging system) and for typical MWIR and LWIR warning sensors. Turbulence MTF were calculated for a slant path of 5 km from the ground to a height of 100 m for upward and downward looking cases. For horizontal paths at a height of 2 m and 30 m the resolution limits due to turbulence were compared with the corresponding diffraction-limited ones. Calculations of the normalized intensity fluctuations were carried out for two slant propagation paths (zenith angle $\beta = 30°$ and 80°).

Keywords: atmospheric turbulence, structure parameter of index of refraction C_n^2, scintillation, aperture averaging, turbulence modulation transfer function MTF, point spread function PSF, spatial resolution.

1. INTRODUCTION

One of the most important effects of atmospheric turbulence on electro-optical systems is the induced degradation of system resolving power. The structure constant of refractive index fluctuations, C_n^2, is the parameter most commonly used to describe the atmospheric turbulence.

Atmospheric turbulence causes intensity fluctuations, or scintillation, in the receiver focal plane which affect the signal to noise ratio of the sensors and reduce the spatial resolution. The modulation transfer function, MTF, is commonly used to describe the resolving power of a sensor as a function of the spatial frequency. The corresponding turbulence point spread function, PSF, represents the turbulence-induced spatial irradiance distribution of a point source in the detector plane. The standard deviation of the PSF, indicating the spatial resolution of the system can easily be derived from the MTF. The spatial resolution of electro-optical systems is limited by atmospheric turbulence and by diffraction of the optic. Prediction of turbulence MTF or the standard deviation of the corresponding PSF is important for cost-effective design, since it permits sensor selection based on the turbulence MTF, which is often the weakest link in imaging systems through the atmosphere. Enlarging the aperture diameter of the sensor optic would improve the diffraction-limited spatial resolution of the system, but this would only be suggestive for those cases where the expected turbulence-limited spatial resolution is better than the diffraction-limited resolution; e.g., smaller values of spatial resolution.

Calculations were performed for military relevant IR sensors, for a SWIR sensor, wavelength 1.57 µm, a MWIR warning sensor, wavelength 4 µm, and a LWIR warning sensor, wavelength 10 µm. The selected C_n^2 values correspond to a cumulative frequency of occurrence of 90 % measured during daytime at noon in arid summer (overall strongest turbulence) and mid-European winter (weakest turbulence at noon) and during winter night in mid-Europe (overall weakest turbulence).

e-mail: wrana@fom.fgan.de, Tel: 49-(0)7243-992 118, Fax: 49-(0)743-992 299

Turbulence MTFs were calculated for an upward and downward looking sensor along a slant path of 5 km between the ground and a height of 100 m. According to the height dependence of C_n^2 the turbulence of the downward looking case indicate a significantly better spatial resolution.

For a horizontal path close to the ground one expects the strongest influence of turbulence on electro-optical systems. The resolution limits due to turbulence were calculated for each sensor assuming a height of 2 m (tank) and 30 m (helicopter). These calculations were performed for the selected C_n^2 values and were compared with the corresponding diffraction-limited resolution.

The expected normalized aperture-averaged intensity fluctuations were calculated for slant paths with zenith angle $\beta = 30°$ and 80°. Based on the response at shorter wavelengths, the expected intensity fluctuations for the SWIR sensor are significantly larger than those of the IR warning sensors. For the worst case, at noon during arid summer, strong scintillation may cause difficulties for the subsequent signal processing.

2. THEORY

2.1 Height profile of C_n^2

Values of C_n^2 can be scaled according to various models of the height profile of C_n^2. Experiments up to 100 m elevation support primarily the models of

Tatarski[1] $C_n^2(h) = C_{n0}^2 \cdot h^{-4/3}$ during day (1)

$C_n^2(h) = C_{n0}^2 \cdot h^{-2/3}$ during night

and Brookner[2] $C_n^2(h) = C_{n0}^2 \cdot h^{-5/6} \cdot \exp(-h/h_0)$, (2)

where C_{n0}^2 is the value at the surface and h_0 is 320 m.

Above the boundary layer (up to about 1000 m during daytime) the most commonly used C_n^2 profile model is the Hufnagle-Valley (H-V) model. Andrews [3] described C_n^2 using a modified H-V model, taking into account the C_{n0}^2 value at the surface:

$$C_n^2 = 0.00594(v/27)^2 \cdot (10^{-5} h)^{10} \cdot \exp(-h/1000) + 2.7 \cdot 10^{-16} \cdot \exp(-h/1500) + C_{n0}^2 \cdot \exp(-h/100), \quad (3)$$

where h is in m and v is the wind speed in ms^{-1}.

2.2 Turbulence Modulation Transfer Function MTF and Point Spread Function PSF

The MTF yields a quantitative estimate for degradation of a target resolution of an electro-optical system. The contribution of atmospheric turbulence to the time dependent MTF of an imaging system is given by Azoulay[4] to be:

$$MTF_{TURB}(\xi, \tau) = exp\left[-\left[\frac{\lambda \xi}{\rho_p(\tau)} \right]^{5/3} \right] \quad (4)$$

with spatial frequency ξ and wavelength λ where the time dependent effective transverse coherence length $\rho_p(\tau)$ is given by:

$$\rho_0(\tau) = \rho_0 \left[1 + 0.37 \cdot \left[\frac{\rho_0}{D_0 + v_t \cdot \tau} \right]^{1/3} \right] \quad (5)$$

with the transverse coherence length ρ_0 and the effective aperture diameter $D(\tau) = D + v_t \cdot \tau$, where v_t is the crosswind velocity and τ the exposure time.

For a horizontal path, where C_n^2 is constant along the path length L, the transverse coherence length ρ_0 is given by:

$$\rho_0 = \left[21.614 \cdot C_n^2 \frac{L}{\lambda^2} \right]^{-3/5}. \quad (6)$$

For a slant path, where C_n^2 is a function of height, the path-integrated transverse coherence length ρ_0 along the path length L, where $L = H \cdot \sec \beta$ with zenith angle β, is given for a spherical wave by [5]:

for downward looking case (sensor at height H, source at the ground)

$$\rho_0 = \left[1.46\,k^2 \cdot \sec(\beta) \cdot \int_0^H C_n^2(h) \cdot \left(\frac{h}{H}\right)^{5/3} dh\right]^{-3/5} \tag{7}$$

for upward looking case (sensor at the ground, source at height H)

$$\rho_0 = \left[1.46\,k^2 \cdot \sec(\beta) \cdot \int_0^H C_n^2(h) \cdot \left(\frac{H-h}{H}\right)^{5/3} dh\right]^{-3/5}. \tag{8}$$

Turbulence close to the sensor does affect the transverse coherence length ρ_0 more than turbulence far from the receiver.

The PSF indicates the spatial irradiance distribution of a point source in the detector plane. Assuming no phase shift the PSF can be calculated by applying the inverse Fourier transformation to the MTF:

$$PSF(x,y) = F^{-1}\left[MTF(\xi)\right]. \tag{9}$$

The standard deviation of the PSF, σ_{PSF}, is used to describe the degradation of the spatial resolution of the sensor due to atmospheric turbulence and can be calculated by fitting the MTF to a Gauss Function

$$MTF_{Fit} = \exp\left(-\left(\frac{\lambda\xi_f}{\rho_p}\right)^{5/3}\right) = \exp\left(-2\pi^2\,\sigma_{PSF}{}^2\,\xi_f{}^2\right) = \frac{1}{\sqrt{e}}$$

$$\sigma_{PSF} = \frac{1}{2\pi \cdot \xi_f} \tag{10}$$

The turbulence-induced limitation in resolution α_{turb} is calculated by: $\alpha_{turb} = 2 \cdot \sigma_{PSF}$ (11)

For comparison the resolution limit due to diffraction α_{optic} is calculated by: $\alpha_{optic} = \frac{1.22 \cdot \lambda}{D}$ (12)

2.3 Normalized Aperture Averaged Intensity Fluctuation, Scintillation

Atmospheric turbulence also causes intensity fluctuations, scintillation, in the receiver focal plane which affect the signal to noise ratio of warning sensors. The variance of the log amplitude fluctuations, σ_A^2, can be related to C_n^2.

For a slant path C_n^2 σ_A^2 can be calculated for a spherical wave by [5]

for downward looking case (sensor at height H and source at the ground)

$$\sigma_A^2(L) = 0.56 \cdot k^{7/6} \cdot (\sec\beta)^{11/6} \cdot \int_0^H C_n^2(h) \cdot \left(\frac{h}{H}\right)^{5/6} \cdot (H-h)^{5/6} \cdot dh \tag{13}$$

for upwards looking case (sensor at the ground and source at height H)

$$\sigma_A^2(L) = 0.56 \cdot k^{7/6} \cdot (\sec\beta)^{11/6} \cdot \int_0^H C_n^2(h) \cdot \left(\frac{H-h}{H}\right)^{5/6} \cdot h^{5/6} \cdot dh\,, \tag{14}$$

with $k = 2\pi/\lambda$. Path weighting of C_n^2 for scintillation favours turbulence far from the receiver. Generally speaking, turbulence near the receiver does not contribute to scintillation. The wavelength dependence of σ_A^2 indicates a general feature of turbulence effects: turbulence effects are greater for shorter wavelengths.

The normalized intensity variance σ_I^2 is defined by $\sigma_I^2 = \frac{\left\langle \left[I - \langle I \rangle\right]^2 \right\rangle}{\langle I \rangle^2}$,

and satisfies $\sigma_I^2 = \exp(4\sigma_A^2) - 1.$ (15)

This formula can be applied for larger zenith angles as long as the variance of log amplitude does not become larger than the limit imposed by the Rytov approximation, $\sigma_A^2 < 0.3$. In agreement with the Rytov approximation the variance increases linearly with C_n^2 only for low levels of turbulence. For higher levels the experimental variance approaches a constant and indeed decreases slightly for still higher levels of turbulence. This behaviour is known as the saturation of scintillation.

For strong path-integrated turbulence, approximate expressions for calculation of the variance of normalized intensity fluctuations were derived by Churnside [6]:

$$\sigma_I^2 = 1 + 3.86\left(\frac{k\cdot\rho_0^{\,2}}{L}\right)^{1/3}. \qquad (16)$$

The description of scintillation effects in weak turbulence has been confined to point sources and to point detectors. If the aperture D of an detector is larger than the Fresnel zone, $D > 2(L/k)^{1/2}$, the detector will average fluctuations over the aperture, and the signal fluctuation will be less than those from a point receiver. The aperture averaging factor A is defined as the ratio of the normalized variance of intensity fluctuations from a receiver with aperture diameter D, $\sigma_{I(D)}^2$, to that from a detector with infinitesimally small aperture σ_I^2.

Approximate expressions for A for a spherical wave were derived by Churnside [6]

for week path-integrated turbulence

$$A = \sigma_{I(D)}^2 / \sigma_I^2 = \left[1 + 0.214\left(\frac{kD^2}{4L}\right)^{7/6}\right]^{-1} \qquad (17)$$

for strong path-integrated turbulence

$$A = \frac{\sigma_I^2+1}{2\cdot\sigma_I^2}\left[1+0.908\left(\frac{D}{2\rho_0}\right)^2\right]^{-1} + \frac{\sigma_I^2-1}{2\cdot\sigma_I^2}\left[1+0.613\left(\frac{kD\rho_0}{2L}\right)^{7/3}\right]^{-1} \qquad (18)$$

with the transverse coherence length ρ_0. The factor A increases with increasing wavelength; therefore, for the same aperture diameter the averaging effect is larger in MWIR than in LWIR.

3. C_n^2 MEASUREMENTS IN ARID CLIMATE AND IN MID-EUROPE

Temperature and humidity fluctuations are known to be the primary mechanism affecting the index of refraction and thus the atmospheric turbulence. In daytime the solar radiation warms up the ground and the air. The temperature gradient between ground and atmosphere results in an turbulent vertical air stream. Higher ground temperature usually leads to larger temperature gradient and hence to stronger turbulence. The temperature gradient is generally greatest at midday when the ground is warmer than the overlying air, thus increasing C_n^2. Surface roughness increases the temperature gradient and thus C_n^2. Wind causes air mixing and therefore decreases the inhomogeneity of temperature and humidity and hence decreases C_n^2. Increasing wind also enhances the dissipation of ground heating, which causes decreasing temperature gradient and C_n^2. The strength of atmospheric turbulence depends on the net radiation which is sensitive to cloudiness. When the air temperature is closest to the ground temperature, mainly at sunrise, C_n^2 has a minimum value. During night there is no heating of the ground and the air, the temperature gradient is smaller and hence the vertical heat flux decreases. In the case of laminar temperature flux (horizontal flux) the C_n^2 values are very low. If the temperature of the ground is lower than the air wind causes vertical temperature flux which results in turbulent flux and strong turbulence of short duration. This results in a strong oscillation of C_n^2 values, an effect that is called intermittence. Higher wind velocity increases this effect. Intermittence can mainly be observed during winter nights and over snow covered ground. The strength of turbulence was classified in the following way:

very weak turbulence:	$C_n^2 < 6\cdot10^{-16}$ m$^{-2/3}$
weak turbulence:	$6\cdot10^{-16}$ m$^{-2/3}$ < C_n^2 < $6\cdot10^{-15}$ m$^{-2/3}$
medium turbulence:	$6\cdot10^{-15}$ m$^{-2/3}$ < C_n^2 < $6\cdot10^{-14}$ m$^{-2/3}$
strong turbulence:	$6\cdot10^{-14}$ m$^{-2/3}$ < C_n^2 < $6\cdot10^{-13}$ m$^{-2/3}$
very strong turbulence:	$6\cdot10^{-13}$ m$^{-2/3}$ < C_n^2

Measurements of C_n^2 values were performed with two identical laser scintillometers in moderate climate, mid-Europe, Germany, and in arid climate over an optical path length of 100 m. All data were collected continuously for a period of at least one year at a time resolution of 5 minutes. The measurements are described in detail in Weiss-Wrana and Balfour [7].

3.1 Diurnal cycle of C_n^2 values

Examples of the C_n^2 values measured during an arbitrary chosen summer month in arid climate (strongest turbulence) and winter month in moderate climate (weakest turbulence) are plotted in Figure 1.

In arid climate the weather conditions were constant. During summer season there was no overcast sky and the ground was totally dry. All days show the same characteristic diurnal cycle of C_n^2. Around noon the atmospheric turbulence was strongest, rising to values of about $2 \cdot 10^{-12}$ $m^{-2/3}$. In the early morning around sunrise when the temperature stratification of the atmosphere is stable, the daily variation indicates a distinguished minimum of C_n^2 with values of about $2 \cdot 10^{-15}$ $m^{-2/3}$. During winter season the lower solar irradiance leads to lower ground temperature and the maximum of C_n^2 is reduced to values $\leq 1 \cdot 10^{-12}$ $m^{-2/3}$. The midday maximum change by a factor of about 2.5 during the year. During the day the overcast sky reduces the temperature gradient and hence C_n^2 values. Clouds will lead to a 1-2 magnitude reduction in the midday magnitudes. The diurnal cycles indicate a significant variability of the C_n^2 values due to changing cloudiness, but the characteristic diurnal pattern can still be recognized. For more details see Weiss-Wrana and Balfour [7].

In mid-Europe the weather situation can significantly change during a short time period. Due to the weather variability in mid-Europe the C_n^2 values show large variance. Nevertheless the characteristic pattern of the daily variation is perceptible during summer. Winter season here is quite different from winter season in the arid climate. Air temperature is significantly lower, causing a very small temperature gradient and hence weak turbulence even during sunny days. Most of the C_n^2 values are $< 1 \cdot 10^{-13}$ $m^{-2/3}$. Intermittence is likely which results in oscillating C_n^2 values, hence singular large C_n^2 values up to $2 \cdot 10^{-12}$ $m^{-2/3}$, corresponding to very strong turbulence, could appear. The characteristic diurnal pattern is no longer identifiable.

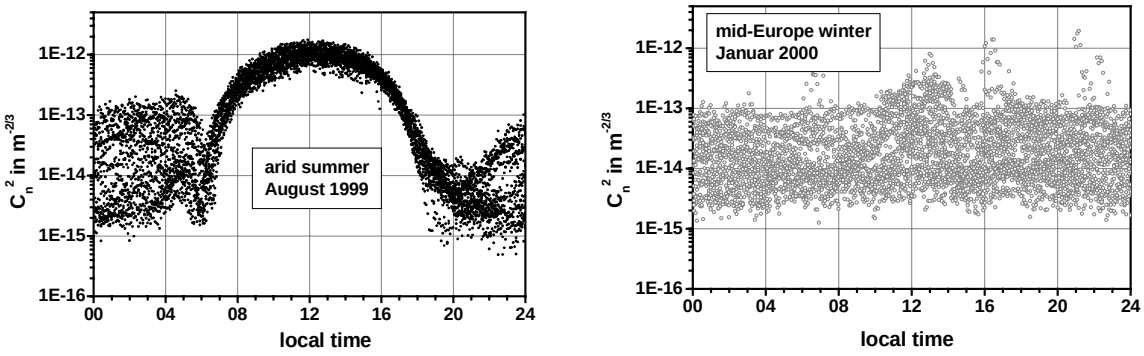

Figure 1: Diurnal cycle of C_n^2 values measured during a time period of one month in summer in arid climate (left graph), and one winter month in moderate climate, mid-Europe (right graph).

3.2 Cumulative frequency of occurrence of C_n^2 values

Since the atmospheric parameters and hence the atmospheric turbulence usually change as a function of time-of-day and of season their influence on the effectiveness of electro-optical systems can normally only be expressed in a statistical way. To provide a statistical data base for atmospheric turbulence, the cumulative frequency of occurrence was calculated for a time period of one month for both climates. As an example for highest and lowest atmospheric turbulence strength, one summer and one winter month in both climates were selected and analysed. Results of the cumulative frequency of occurrence based on the complete data set of 24 hours (full day) were discussed in details in Weiss-Wrana and Balfour [7].

As the diurnal run of C_n^2 values varies by more than one decade, the calculation of turbulence effects demands a more differentiated statement on the expected atmospheric turbulence strength versus the time of day. The cumulative frequency of occurrence was calculated for two-hours time intervals during three selected times of the day: during daytime around noon (11:00 – 13:00 local time), during night time around midnight (0:00 – 2:00 local time) and around sunrise. The results for moderate climate in mid-Europe and arid climate were plotted in Figure 2.

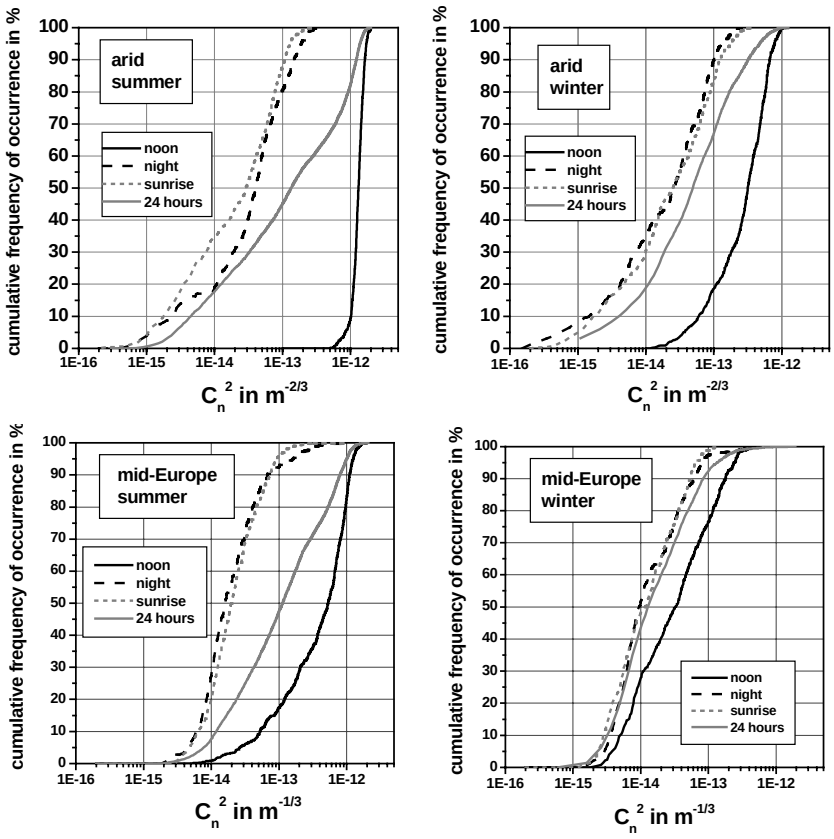

Figure 2: Cumulative frequency of occurrence of C_n^2 values measured in two climates for a time period of one month during different seasons (summer and winter) and during different time of day (noon, midnight, sunrise).
upper graph: arid climate, lower graph: moderate climate, mid-Europe.

The C_n^2 values corresponding to a cumulative frequency of occurrence of 90 % are listed in Table 1. During daytime (around noon) these C_n^2 values vary between 1.8 10^{-13} $m^{-2/3}$ (strong turbulence) in mid-European winter and $1.6 \cdot 10^{-12}$ $m^{-2/3}$ (very strong turbulence) in arid summer. During night the measured C_n^2 values do not indicate such a significant difference. It should be mentioned that the statistical analyses of the night time data yields to larger C_n^2 values than one might expect. This has to be taken into account for estimation of sensor performance limitation.

climatic conditions		**C_n^2-values (in $m^{-2/3}$) corresponding to cumulative frequency of occurrence of 90 %**			
climate	**season**	**full day 24 hours**	**noon 11:00 – 13:00**	**night 0:00- 02:00**	**sunrise**
moderate mid-Europe	**summer**	$7.9 \cdot 10^{-13}$	$1.1 \cdot 10^{-12}$	$7.4 \cdot 10^{-14}$	$6.7 \cdot 10^{-14}$
	winter	$8.3 \cdot 10^{-14}$	**$1.8 \cdot 10^{-13}$**	**$5.4 \cdot 10^{-14}$**	$6.3 \cdot 10^{-14}$
arid	**summer**	$1.2 \cdot 10^{-12}$	**$1.6 \cdot 10^{-12}$**	$1.5 \cdot 10^{-13}$	$1.1 \cdot 10^{-13}$
	winter	$3.2 \cdot 10^{-13}$	$6.7 \cdot 10^{-13}$	$1.0 \cdot 10^{-13}$	$6.7 \cdot 10^{-13}$

Table 1: C_n^2 values corresponding to a cumulative frequency of occurrence of 90 % measured during different times of the day during two different seasons in two different climates, arid climate and moderate climate, mid-Europe.

The corresponding C_n^2 values measured during strongest daytime turbulence, $C_n^2 = 1.6 \cdot 10^{-12}$ $m^{-2/3}$ (arid summer at noon), and weakest daytime turbulence, $C_n^2 = 1.8 \cdot 10^{-13}$ $m^{-2/3}$ (mid-Europe winter at noon), and weakest night time turbulence, $C_n^2 = 5.4 \cdot 10^{-14}$ $m^{-2/3}$ (mid-Europe winter at midnight) were selected and applied for the following calculations in sections 4 and 5.

4. CALCULATION OF TURBULENCE MTF AND SPATIAL RESOLUTION

Prediction of the turbulence MTF is important for cost-effective design, since it permits sensor selection based on the turbulence MTF, which often is the weakest link in imaging systems through the atmosphere. Calculations of turbulence MTFs were performed for three selected C_n^2 values for the following IR sensors:

SWIR sensor (active imaging system): wavelength λ = **1.57 µm**, aperture diameter 125 mm, exposure time 0.1 ms,
MWIR warning sensor: wavelength λ = **4 µm**, aperture diameter 200 mm, exposure time 1 ms,
LWIR warning sensor: wavelength λ = **10 µm**, aperture diameter 200 mm, exposure time 0.1 ms.

4.1 Turbulence MTF for a slant path

The expected turbulence MTFs were calculated for a 5 km slant path, between the ground and a height of 100 m, for upward looking (sensor on a helicopter, target on the ground) and downward looking (sensor on the ground, target at a height of 100 m) case. The corresponding turbulence MTFs are plotted in Figure 3.

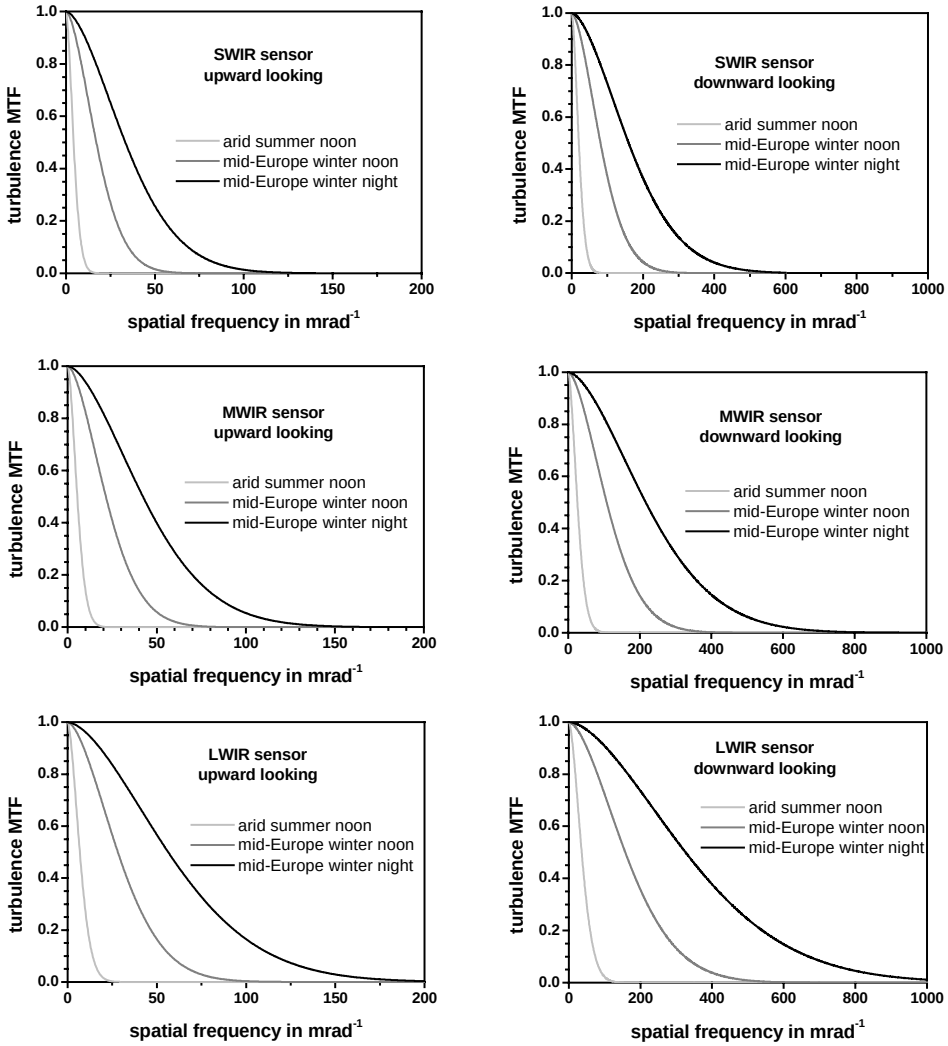

Figure 3: Turbulence MTF calculated for SWIR sensor (upper graphs), MWIR sensors (middle graph) and LWIR sensor (lowest graph) for three selected C_n^2 value along a slant path upward looking (left graphs) and downward looking (right graphs).

It is evident that the turbulence MTFs calculated for the downward looking case (right graphs) show a significant broader feature and better spatial resolution than the MTF for the upward looking case (left graphs). Based on the longer wavelength response the spatial resolution of a LWIR warning sensor is better than that of a MWIR warning sensor or a SWIR sensor. Each graph demonstrates the seasonal and climatic variation of the turbulence MTF, e.g. the turbulence MTF expected around noon in arid summer (light grey line) and mid-European winter (grey line). Each graph also indicates the variation of MTF expected for different times of the day in mid-European winter, for midnight hours (black line) and midday hours (grey line). For summer conditions in mid-Europe and arid climate one would expect an even larger difference.

4.2 Comparison of turbulence-limited and diffraction-limited resolution for horizontal paths

The spatial resolution of electro-optical systems is limited by atmospheric turbulence and by diffraction of the optic. Cost-effective design of warning sensors demands information of the expected turbulence-limited and the diffraction-limited spatial resolution of the sensor. The turbulence-limited resolution, α_{turb}, i.e. the standard deviation of the PSF, σ_{PSF}, can easily be derived from the turbulence MTF, Eq. (10) and Eq. (11). Enlarging the aperture diameter of the sensor optic would improve the diffraction-limited spatial resolution of the system, but this would only be effective as long as the expected turbulence-limited resolution $\alpha_{turb} < \alpha_{opt}$.

Calculations of σ_{PSF} were performed for all three systems for the selected three turbulence strengths for a horizontal path at heights of 2 m and 30 m above ground (systems mounted on a tank and on a helicopter). Assuming a flat area, the maximum geometrical horizon at a height of 2 m would be 5 km and 19.5 km at a height of 30 m. Tatarsky´s model was applied for height scaling of C_n^2. The detection range of the SWIR sensor was assumed to be 5 km and that of IR warning sensors (third generation) to be 20 km. For comparison the resolution limit due to diffraction was calculated.

Figure 4 demonstrates the results for the SWIR sensor (upper graphs), the MWIR Warning sensor (middle graph) and the LWIR warning sensor (lowest graph) for a height of 2 m (left graphs) and 30 m above ground (right graphs). It is obvious that due to the height scaling of C_n^2, atmospheric turbulence decreases much stronger the limit of spatial resolution at lower altitudes, e.g. 2 m (left graphs), than at higher altitudes, e.g. 30 m (right graphs). For the LWIR sensor the turbulence-limited resolution is slightly better than that for the SWIR sensor but the diffraction-limited resolution is significantly worse. The results are summarized in Table 2. It should be pointed out that these results are sensitive to the accuracy of height scaling of C_n^2.

	limitation of spatial resolution			
sensor	height	arid summer noon $C_n^2 = 1.6 \cdot 10^{-12}\ m^{-2/3}$	mid-Europe winter noon $C_n^2 = 1.8 \cdot 10^{-13}\ m^{-2/3}$	mid-Europe winter night $C_n^2 = 5.4 \cdot 10^{-14}\ m^{-2/3}$
SWIR senor λ = 1.57 µm	2 m 30 m	turbulence turbulence	turbulence > 4 km turbulence	turbulence diffraction
MWIR sensor λ = 4 µm	2 m 30 m	turbulence > 2.7 km turbulence	turbulence diffraction	turbulence diffraction
LWIR sensor λ = 10 µm	2 m 30 m	turbulence > 17 km turbulence	> 4 km turbulence diffraction	diffraction diffraction

Table 2: Comparison of the resolution limit due to atmospheric turbulence and diffraction for a SWIR, MWIR and LWIR sensor along a horizontal path at a height of 2 m and 30 m, as expected for different turbulence strength as measured .

An improvement of spatial resolution by enlarging the aperture diameter might be sufficient for some cases:
for example in mid-Europe for short distance applications at higher altitudes and additionally for LWIR sensors at lower altitudes during winter nights.

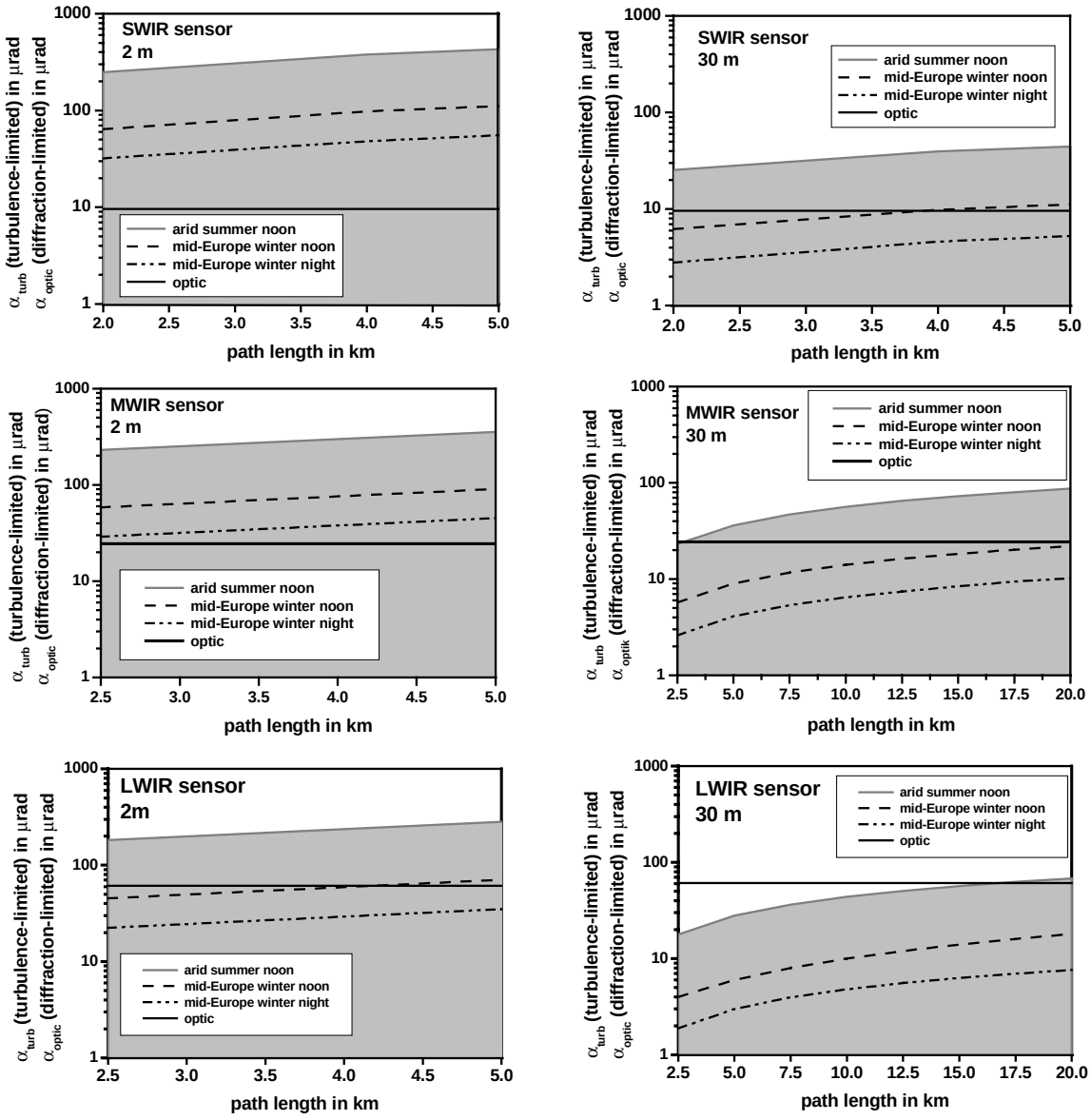

Figure 4: Diffraction and turbulence-limited resolution for three IR sensors:
SWIR sensor (upper graphs), MWIR sensors (middle graph) and LWIR sensor (lowest graph) along a horizontal path at a height of 2 m (left graphs) and at 30 m (right graphs) for selected C_n^2 values.

5. CALCULATION OF THE EXPECTED NORMALIZED INTENSITY FLUCTUATION OF DIFFERENT IR-SENSORS

The intensity variance is a readily observable quantity and is important for the subsequent signal processing of electro-optical sensors. The variance of aperture-averaged normalized intensity fluctuation $\sigma_{I(D)}^2 = A \cdot \sigma_I^2$ was calculated for the SWIR sensor with D = 125 mm, for the MWIR warning sensor and for the LWIR warning sensor with D = 200 mm. The calculations were carried out for slant paths with different zenith angles, $\beta = 30°$ and 80 for the selected turbulence conditions for path lengths up to 5 km in the case of the SWIR sensor (active imaging system) and up to 20 km in the case of the MWIR and LWIR warning sensors. The selected C_n^2 values correspond to the cumulative frequency of

occurrence of 90 % measured during strongest daytime turbulence, $C_n^2 = 1.6 \cdot 10^{-12}$ $m^{-2/3}$ (arid summer at noon) and weakest daytime turbulence, $C_n^2 = 1.8 \cdot 10^{-13}$ $m^{-2/3}$ (mid-Europe winter at noon) and during weakest night time turbulence, $C_n^2 = 5.4 \cdot 10^{-14}$ $m^{-2/3}$.

System design demands information about expected intensity fluctuations, $\sigma_{I(D)}$. The resulting normalized aperture-averaged intensity fluctuations, $\sigma_{I(D)}$, are plotted in Figure 5.

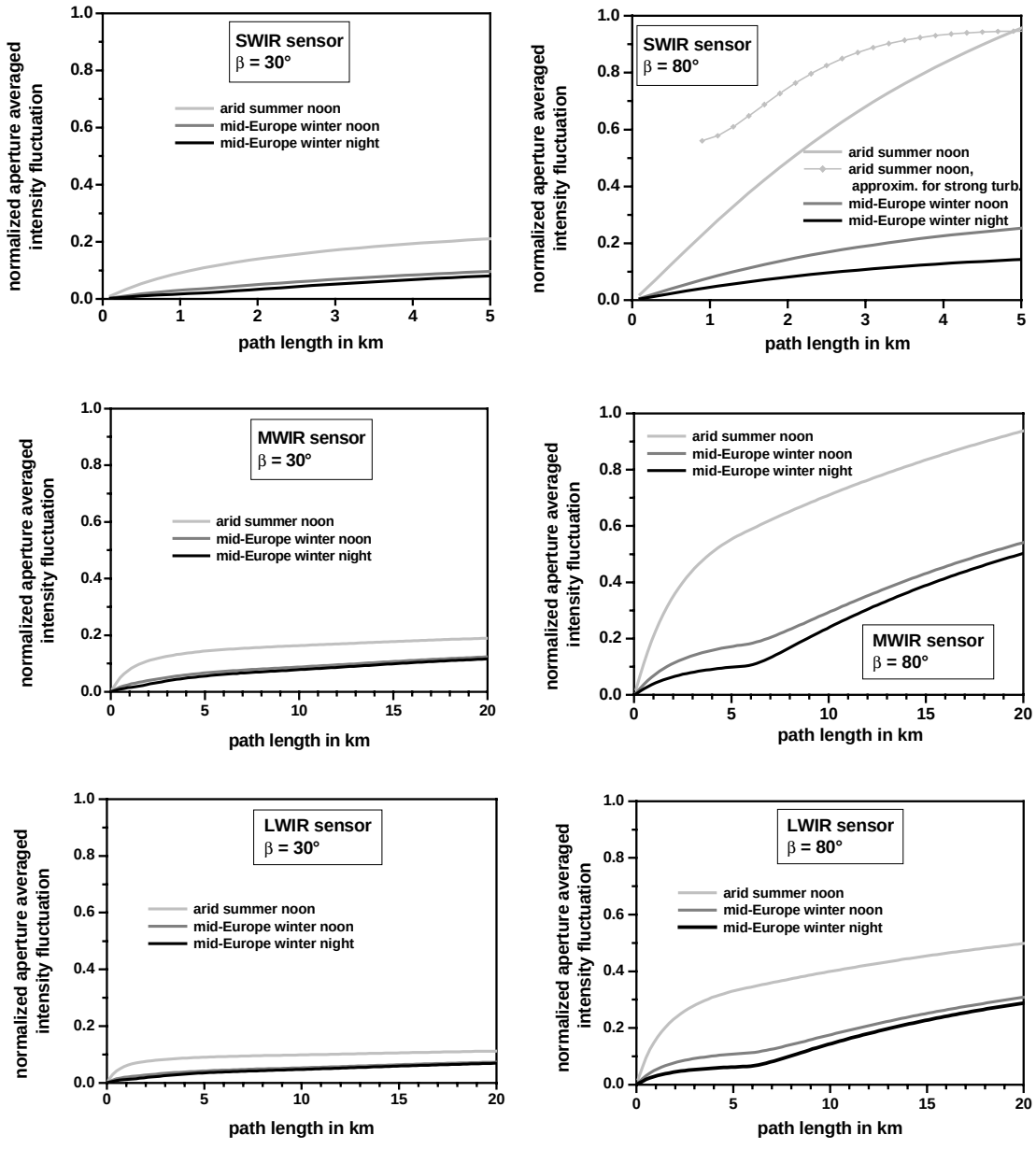

Figure 5: Normalized aperture-averaged intensity fluctuation calculated for three IR sensors: SWIR sensor (upper graphs), MWIR sensor (middle graph) and LWIR sensor (lowest graph) along a slant path with zenith angle β = 30° (left graphs) and 80° (right graphs) for three selected C_n^2 values.

In the case of a steep slant path, $\beta = 30°$, one would expect moderate intensity fluctuations. Under strongest turbulence conditions, like at noon in arid summer, the intensity fluctuation of the SWIR sensor along a 5 km path length is expected to be 0.2. The intensity fluctuations of the MWIR and LWIR sensors along a 20 km path length are expected to be 0.19 and 0.11, respectively.

In the case of a flat slant path, $\beta = 80°$, the path integrated C_n^2 values will be larger according to the height scale of C_n^2. Under strongest turbulence conditions (arid summer at noon) the approximations for strong turbulence had to be applied for the SWIR sensor. Saturation will occur at a path length of about 5 km with maximum intensity fluctuation of 0.94 whereas for the turbulence conditions at noon in mid-European winter the formula for weak turbulence could still be used. The corresponding intensity fluctuations are expected to be 0.25 and 0.14, respectively during the night in mid-European winter. Turbulence effects are smaller for longer wavelengths. For the MWIR and LWIR sensor the formula for weak turbulence could be applied even for path lengths up to 20 km. Under strongest turbulence conditions one expects very strong intensity fluctuations up to 0.94 for the MWIR sensor and strong intensity fluctuations up to 0.49 for the LWIR sensor. Such strong intensity fluctuations may limit the effectiveness of the IR sensors and have to be taken into account for subsequent signal processing.

The results are sensitive to the height scaling of C_n^2. For a height up to 1000 m, Brookner´s formula [2] was applied, for heights > 1000 m the modified H-V model [3] was used.

6. CONCLUSION

During long-term experiments FGAN-FOM measured C_n^2 values over land in two different climates, in moderate climate, mid-Europe and in arid climate. The statistical analysis of the measured C_n^2 values was extended to a more differentiated statement of the cumulative frequency of occurrence during different times of the day. For a summer and a winter month the cumulative frequency of occurrence was determined for two-hours time intervals around noon, midnight and sunrise. The selected C_n^2 values correspond to a cumulative frequency of occurrence of 90 % as measured during daytime at noon in arid summer (overall strongest turbulence, $C_n^2 = 1.6 \cdot 10^{-12}$ $m^{-2/3}$) and mid-European winter (weakest turbulence at noon, $C_n^2 = 1.8 \cdot 10^{-13}$ $m^{-2/3}$) and during night in mid-European winter (overall weakest turbulence, $C_n^2 = 5.4 \cdot 10^{-14}$ $m^{-2/3}$). It should be mentioned that the statistical analysis of the night time data yields larger C_n^2 values than one might expect. This has to be taken into account for the estimation of sensor performance limits.

The selected C_n^2 values were applied to calculate the turbulence effects on three IR sensors: a SWIR sensor (wavelength 1.57 µm, aperture diameter 125 mm, active imaging system), a MWIR warning sensor (wavelength 4 µm, aperture diameter 200 mm) and a LWIR warning sensor (wavelength 10 µm, aperture diameter 200 mm).

Turbulence MTFs were calculated for a 5 km slant path between the ground and a height of 300 m for upward looking sensors (sensor on the ground, source at 300 m height, e.g. helicopter) and downward looking sensors (sensor at a height of 300 m, e.g. on a helicopter, source at the ground, e.g. tank) for the selected C_n^2 values. For downward looking sensors the spatial resolution is significantly better than for the upward looking ones, according to the path weighting of C_n^2. The features of the MTFs calculated for the turbulence strength typical for midnight hours and midday hours differ significantly and so do the MTFs calculated for the turbulence strength measured during the same time of day in different seasons and climates.

The limit of spatial resolution due to turbulence was calculated for horizontal paths at a height of 2 m (sensor on a tank) and 30 m (sensor on a helicopter) and compared with the corresponding diffraction-limited resolution. Resolution degradation caused by atmospheric turbulence is only slightly improved at larger wavelengths, but the resolution degradation is significantly worse at longer wavelengths (assuming the same aperture diameter). At a height of 2 m, turbulence always limits the spatial resolution of SWIR and MWIR sensors, whereas in the case of the LWIR sensor, diffraction would limit the resolution during night and at noon during mid-European winter for short path lengths, < 4 km. At a height of 30 m only very strong turbulence (at noon in arid summer) limits the resolution of the SWIR and MWIR sensors An improvement of spatial resolution by enlarging the aperture diameter might be possible in mid-Europe for short distance applications at higher altitude and additionally for LWIR sensors at low altitudes during the winter.

The normalized aperture averaged intensity fluctuations were calculated for a steep and a flat slant path with zenith angle $\beta = 30°$and $\beta = 80°$. Along the steep path, moderate intensity fluctuations up to 20 % have to be expected. Along the flat slant path very strong intensity fluctuations up to 94 % have to be expected. In the case of the SWIR sensor the approximation for strong turbulence had to be applied. Such strong intensity fluctuations may limit the effectiveness of the IR sensors and have to be taken into account for subsequent signal processing.

It should be mentioned that these results are sensitive to the height scaling of C_n^2.

7. REFERENCES

1. Tatarski V.I.: *Wave Propagation in a Turbulent Medium*, McGraw-Hill Book C. Inc., New York, 1961.
2. Brookner E.: "Improved Model for the Structure Constant variations with Altitude", *Appl. Opt.*, **Vol. 10**, pp. 1960-1962, 1971.
3. Andrews L., Phillips R., Hopen C.: *Laser Beam Scintillation with Applications*, SPIE PRESS, Bellingham, Washington, 2001.
4. Azoulay E.: "Effects on Atmospheric Turbulence on the MTF of Imaging Systems", Bericht FGAN-FfO 1990/3.
5. Beland R.R.: "Propagation through Atmospheric Optical Turbulence", *The Infrared & Electro-Optical Systems Handbook, Volume 2: Atmospheric Propagation of Radiation*, Smith Editor, SPIE Optical Engineering Press, Bellingham, Washington, 1993.
6. Churnside J.: "Aperture Averaging of Optical Scintillation in the Turbulent Atmosphere", *Appl. Opt.*, **Vol.30**, pp.1982-1993, 1991.
7. Weiss-Wrana K.R., Balfour L.: "Statistical Analysis of Measurements of Atmospheric Turbulence in Different Climates", SPIE Proceedings Series, Vol. 4538, pp. 93 – 101, 2002. Bericht FGAN-FOM 2001/20.